

Chk1 and Wee1 kinases coordinate DNA replication, chromosome condensation, and anaphase entry

Barbara Fasulo^a, Carol Koyama^a, Kristina R. Yu^{a,*}, Ellen M. Homola^b, Tao S. Hsieh^c, Shelagh D. Campbell^b, and William Sullivan^a

^aSinsheimer Laboratories, Department of Molecular, Cellular and Developmental Biology, University of California, Santa Cruz, Santa Cruz, CA 95064; ^bBiological Sciences, University of Alberta, Edmonton, AB T6G 2E9, Canada;

^cDepartment of Biochemistry, Duke University Medical School, Durham, NC 27710

ABSTRACT Defects in DNA replication and chromosome condensation are common phenotypes in cancer cells. A link between replication and condensation has been established, but little is known about the role of checkpoints in monitoring chromosome condensation. We investigate this function by live analysis, using the rapid division cycles in the early *Drosophila* embryo. We find that S-phase and topoisomerase inhibitors delay both the initiation and the rate of chromosome condensation. These cell cycle delays are mediated by the cell cycle kinases *chk1* and *wee1*. Inhibitors that cause severe defects in chromosome condensation and congression on the metaphase plate result in delayed anaphase entry. These delays are mediated by *wee1* and are not the result of spindle assembly checkpoint activation. In addition, we provide the first detailed live analysis of the direct effect of widely used anticancer agents (aclerubicin, ICRF-193, VM26, doxorubicin, camptothecin, aphidicolin, hydroxyurea, cisplatin, mechlorethamine and x-rays) on key nuclear and cytoplasmic cell cycle events.

Monitoring Editor

Julie Brill
The Hospital for Sick Children

Received: Oct 5, 2011

Revised: Jan 4, 2012

Accepted: Jan 10, 2012

INTRODUCTION

Passage through mitosis requires an extensive coordinated reorganization of the chromosomes, nucleus, and cytoplasm. One of the most dramatic events occurs as the cells enter metaphase: the mitotic spindle forms, and the chromosomes condense and align on the metaphase plate. This transition is estimated to require a 10,000- to 20,000-fold compaction of the chromosomes (Woodcock and Ghosh, 2010). The mechanisms driving this process are largely unknown. Pharmacological and genetic analyses reveal that condensins and topoisomerases play key enzymatic roles in driving chromosome compaction. Mutants in structural maintenance of

chromosome protein components, core members of the condensin multimeric complex, result in defects in chromosome condensation as well as segregation (Zhai *et al.*, 2011). Topoisomerase II, an enzyme that catalyzes sealing of DNA breaks, is also essential for proper chromosome condensation and segregation (Coelho *et al.*, 2003). Like condensin, topoisomerase II is part of the chromosome scaffold and has been shown to interact physically with condensin (Cuvier and Hirano, 2003). Both enzymes are believed to participate in the folding and packaging of the mitotic chromosomes. However, little is known about the many additional steps and mechanisms required to package and produce a fully condensed mitotic chromosome.

Studies demonstrate that DNA replication is essential for proper chromosome condensation. Classic experiments in which chromosome condensation is induced prematurely, either through cell fusion or drugs, reveal that chromosomes must be replicated to undergo relatively normal condensation (Johnson and Rao, 1970; Gotoh, 2007). Mechanistic insight into the relationship between DNA replication and chromosome condensation comes from the finding that interactions between topoisomerase II and condensin with chromatin require replicated DNA (Cuvier and Hirano, 2003). Evidence suggests that lengthwise compaction of the chromosomes is determined by the density of the active replication

This article was published online ahead of print in MBcC in Press (<http://www.molbiolcell.org/cgi/doi/10.1091/mbc.E11-10-0832>) on January 19, 2012.

*Present address: The Exploratorium, San Francisco, CA 94123.

Address correspondence to: Barbara Fasulo (fasulo@biology.ucsc.edu).

Abbreviations used: CC2, chromosome condensation 2; ICC1, initiation of chromosome condensation; NEB, nuclear envelope breakdown; NEF, nuclear envelope formation.

© 2012 Fasulo *et al.* This article is distributed by The American Society for Cell Biology under license from the author(s). Two months after publication it is available to the public under an Attribution-Noncommercial-Share Alike 3.0 Unported Creative Commons License (<http://creativecommons.org/licenses/by-nc-sa/3.0>). "ASCB®," "The American Society for Cell Biology®," and "Molecular Biology of the Cell®" are registered trademarks of The American Society of Cell Biology.

origins. High and low densities of active origin recognition complexes (ORCs) are correlated with long, thin or short, fat chromosomes, respectively (Pflumm, 2002). This suggests a model in which fewer active ORCs result in large replication loops generating shorter, thicker chromosomes, whereas more active ORCs produce smaller loops that result in longer and thinner chromosomes (Pflumm and Botchan, 2001).

The dependence of chromosome condensation on proper DNA replication may also be mediated by cell cycle checkpoints. Evidence for involvement of checkpoints comes from studies in mammalian cells in which a delay in the replication of an entire chromosome produces delays in chromosome condensation and results in undercondensed chromosomes at mitosis (Breger *et al.*, 2005). In addition, exposure to cell cycle kinase inhibitors induces inappropriate condensation during S phase (Nghiem *et al.*, 2001). This phenomenon is known as premature chromosome condensation (PCC). Because the kinase inhibitors often used in PCC analysis are broad acting, the specific cell cycle regulators that normally prevent PCC have not been identified (Hatzi *et al.*, 2006). Logical candidates are the S/M checkpoint kinases involved in preventing premature activation of the mitotic kinase Cdk1, thus protecting cells from mitotic catastrophe (Lundgren *et al.*, 1991; Niida *et al.*, 2005). Understanding the mechanism of PCC would have a major effect on cancer treatment because targeting PCC modulators in cells with a compromised S-phase checkpoint would increase their lethality (Nghiem *et al.*, 2001).

It is still unknown whether checkpoints other than the spindle assembly checkpoint ensure proper chromosome congression and alignment on the metaphase plate prior to anaphase entry. A number of studies demonstrate that the presence of damaged DNA during metaphase prevents entry into anaphase (Royou *et al.*, 2005). In some instances this is achieved through activation of the spindle assembly checkpoint (Mikhailov *et al.*, 2002) and in others it is achieved through activation of the Chk1-dependent S-phase/DNA damage checkpoint (Smits *et al.*, 2000; van Vugt *et al.*, 2001; Laurencon *et al.*, 2003; Royou *et al.*, 2010). Whether cell cycle checkpoints also monitor the state of chromosome condensation during metaphase is unclear. Mutations that disrupt chromosome condensation can activate the spindle assembly checkpoint, but this may result from failed microtubule/kinetochore associations (Samoshkin *et al.*, 2009).

Using the rapid division cycles of the early *Drosophila* embryo, we can directly address the relationship between S-phase and chromosome condensation and between chromosome condensation and anaphase entry (Kotadia *et al.*, 2010). In contrast to the 24-h cell cycle of the typical mammalian cell, the syncytial divisions of the *Drosophila* embryo are 15–20 min in length (Kotadia *et al.*, 2010). In spite of their short duration, these cycles possess robust S-phase and spindle checkpoints mediated by conserved checkpoint pathways (Song, 2005). These cycles are well suited for live analysis since they divide synchronously in a monolayer. Inhibitors can be injected at precisely timed stages of the cell cycle and imaged immediately, enabling cause-and-effect relationships to be readily determined. Through a combination of fluorescent probes and green fluorescent protein (GFP) transgenic lines, multiple aspects of the chromosome cycle can be followed in real time, including condensation, alignment on the metaphase plate, and segregation. In addition, zygotic transcription is largely absent during the syncytial divisions (McKnight and Miller, 1976), allowing us to examine the direct effect of the inhibitors on chromosome behavior and cell cycle progression rather than secondary effects due to changes in transcription.

We used S-phase inhibitors (aphidicolin and hydroxyurea), DNA-damaging agents (x-irradiation, cisplatin, and mechlorethamine), and topoisomerase inhibitors (aclerubicin, ICRF-193, VM-26, doxorubicin, and camptothecin) to explore the relationships between DNA replication, chromosome condensation, and anaphase entry. We find S-phase and topoisomerase inhibitors delay both the initiation and rate of chromosome condensation. These delays are mediated by the cell cycle kinases Grp (Chk1) and dWee1 (Wee1). In addition, we show that inhibitors that produce severe defects in chromosome condensation and congression on the metaphase plate also delay anaphase onset. These delays are mediated by dWee1 kinase and are not the result of spindle assembly checkpoint activation.

RESULTS

The nuclear and cytoplasmic effects of cell cycle inhibitors are readily monitored live in *Drosophila* embryos

To examine the effect of DNA inhibitors on cell cycle timing and morphological features, we injected rhodamine-labeled tubulin into *Drosophila* embryos transformed with a histone H2A GFP construct (Clarkson and Saint, 1999; Figure 1 and Supplemental Video S1). This enabled us to simultaneously follow the microtubule-organizing center, spindle, and nuclear envelope formation/breakdown, as well as chromosome morphology and behavior in real time (Yu *et al.*, 2000). We monitored nuclear envelope formation (NEF; Figure 1) at telophase by the exclusion of labeled tubulin from the nucleus. Initiation of chromosome condensation (ICC1; Figure 1) was monitored by the appearance of bright GFP-positive spots in the nucleus. We also defined a second phase of chromosome condensation (CC2; Figure 1) in which the GFP-labeled chromosomes pull away from the nuclear envelope. Nuclear envelope breakdown (NEB) was monitored by labeled tubulin in the cytoplasm flooding into the nucleus (Figure 1). Compaction and alignment of the DNA on the metaphase plate and formation of a mature mitotic spindle were recorded as metaphase (Figure 1, Meta). Separation of sister chromosomes marked the initiation of anaphase (Figure 1, Ana). Live analysis allowed us to determine the timing of the intervals between each of these events. To ensure uniformity in cell cycle timing, all of the described studies were performed on nuclear cycle 12 embryos. Interphase (defined as the interval between NEF and NEB) lasts 9.3 ± 0.7 min. We divided prophase into two intervals: NEF to ICC1, and ICC1 to CC2. These intervals are 3.4 ± 0.5 and 3.0 ± 1.0 min, respectively. Finally, we defined metaphase as the interval between NEB and initiation of anaphase (IA). The length of this interval is 4.1 ± 0.6 min. These results are summarized in Table 1.

To standardize our analysis of the effects of inhibitors on the cell cycle, we injected each inhibitor during metaphase (between NEB and IA) of nuclear cycle 11 and imaged the embryos from telophase of nuclear cycle 11 through telophase of nuclear cycle 12 (Supplemental Figure S1).

For a thorough discussion of the criteria used to obtain a functional equivalence in concentration for the cell cycle inhibitors we injected, see *Materials and Methods*.

Inhibitors that delay S phase increase the interval between NEF and NEB

In the *Drosophila* embryo, the syncytial divisions are very rapid, alternating between interphase and mitosis with extremely short gap phases. Therefore the length of the interval between NEF, at telophase, and NEB, at prophase, is primarily determined by the time it takes to complete S phase (Foe and Alberts, 1983). During the late syncytial cycles interphase becomes progressively longer due

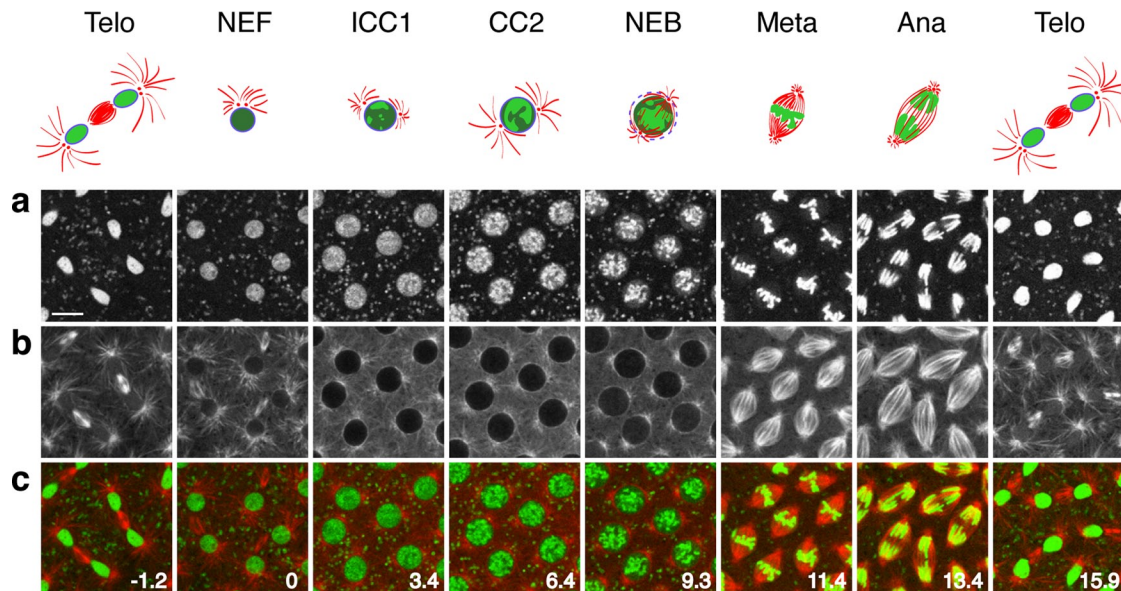


FIGURE 1: Timing syncytial division 12. Images of a syncytial *Drosophila* embryo bearing the histone-GFP construct injected with fluorescently labeled tubulin. Top, cartoon describing the different steps observed in vivo. Starting at telophase of cell cycle 11, the entire cell cycle 12 is shown. Ana, anaphase; CC2, second stage of chromosome condensation; ICC1, initiation of chromosome condensation; Meta, metaphase; NEB, nuclear envelope breakdown; NEF, nuclear envelope formation; Telo, telophase. (A) GFP-histone, (B) rhodamine-tubulin, and (C) merge (GFP-histone in green and rhodamine-tubulin in red). Time is shown in minutes. Scale bar, 8 μ m.

to increasing delays in replication. These delays are due to the introduction of heterochromatin features late in embryogenesis (Shermoen *et al.*, 2010). Like *grp/chk1*-mutant embryos, *dwee1* fails to increase the length of interphase (NEF–NEB) during the late syncytial cycles (Stumpff *et al.*, 2004), suggesting that *dWee1* may also be required for the replication checkpoint.

To establish the effect of S-phase inhibitors on cell cycle timing, we injected the embryos with aphidicolin and hydroxyurea (Figure 2).

The length of interphase (NEF–NEB) was delayed in both aphidicolin- and hydroxyurea-treated embryos (28.4 and 20.5 min, respectively) compared with untreated embryos (9.3 min) (Tables 1 and 2 and Supplemental Videos S2 and S3). However, *dwee1*- and *grp/*

chk1-mutant embryos treated with aphidicolin or hydroxyurea did not show this delay, confirming that *dWee1* is essential for the DNA replication checkpoint (Table 2; Fogarty *et al.*, 1997; Sibon *et al.*, 1997; Price *et al.*, 2000; Shermoen *et al.*, 2010).

We used the length of the NEF–NEB interval to determine whether the DNA-damaging agents x-irradiation, cisplatin, and mechlorethamine produced delays in S phase (Table 1). We exposed embryos to 410 rad of x-irradiation immediately after NEF. Although this dose is strong enough to produce obvious disruptions in chromosome segregation during anaphase, it did not significantly influence the interval between NEF and NEB (9.1 min; Table 1, Figure 3, and Supplemental Videos S4–S6). The most pronounced effect on

	Interphase NEF–NEB	Prophase		
		NEF–ICC1	ICC1–CC2	Metaphase NEB–IA
Wild type (n = 7)	9.3 ± 0.7	3.4 ± 0.5	3.0 ± 1.0	4.1 ± 0.6
+ aphidicolin (n = 5)	28.4 ± 3.7	14.0 ± 2.3	8.4 ± 2.3	7.1 ± 1.2
+ hydroxyurea (n = 4)	20.5 ± 3.3	>8.4	—	>9.0
+ mechlorethamine (n = 3)	12.8 ± 1.7	5.0 ± 0.4	4.7 ± 2.2	6.7 ± 1.6
+ cisplatin (n = 6)	10.3 ± 2.4	5.4 ± 1.2	3.9 ± 1.3	7.4 ± 2.6
+ x-rays (n = 6)	9.1 ± 1.1	3.9 ± 1.2	2.0 ± 0.4	6.5 ± 1.1
+ aclarubicin (n = 3)	11.8 ± 2.1	5.6 ± 0.2	3.4 ± 1.4	7.4 ± 1.1
+ ICRF-193 (n = 10)	10.2 ± 2.1	>5.8	>3.3	7.9 ± 3.3
+ VM26 (n = 6)	11.4 ± 1.8	4.6 ± 0.8	2.10	>10.5
+ doxorubicin (n = 4)	10.0 ± 0.9	4.4 ± 0.5	4.0 ± 1.4	6.6 ± 1.4
+ camptothecin (n = 6)	11.6 ± 1.4	6.1 ± 0.7	2.1 ± 0.7	>7.1

Syncytial nuclear cycle 12 was followed in untreated, drug-treated, and x-irradiated histone-GFP embryos. The following intervals were timed (in minutes): NEF to NEB, NEF to ICC, ICC1 to ICC2, and NEB to IA (see the text). n, number of embryos observed. —, not observed. Values are \pm SD.

TABLE 1: Nuclear cycle timing in drug-treated and untreated embryos.

embryos injected with cisplatin (a DNA cross-linking agent) consisted in chromosome fragments and bridging during anaphase similar to that observed with x-irradiation. Cisplatin did not dramatically increase the length of the interval between NEB and NEF (10.3 min; Table 1). Mechlorethamine also produced significant amounts of chromosome bridging during anaphase (Figure 3). In addition, it produced a slight but significant lengthening in the interval between NEF and NEB (12.8 ± 1.7 vs. 9.3 ± 0.7 min; Table 1). Of note, of the three DNA-damaging agents tested, mechlorethamine is unique in that it cross-links sister DNA strands (Baker *et al.*, 1984).

Topoisomerase II inhibitors (aclarubicin and ICRF-193), topoisomerase II poisons (doxorubicin and VM26), and a topoisomerase I poison (camptothecin) produced pronounced chromosome bridging but relatively minor effects on the length of the NEF-to-NEB interval, indicating that interfering with chromosome condensation does not activate an interphase checkpoint (Figures 4 and 5, Table 1, and Supplemental Videos S7–S11). A visual summary of these findings is provided in Figure 6.

The S-phase inhibitors significantly delay the initiation of chromosome condensation

In untreated embryos, the interval between nuclear envelope formation and the initiation of chromosome condensation (NEF–ICC1) is 3.5 min. Injecting the S-phase inhibitors aphidicolin and hydroxyurea dramatically delayed initiation of chromosome condensation to

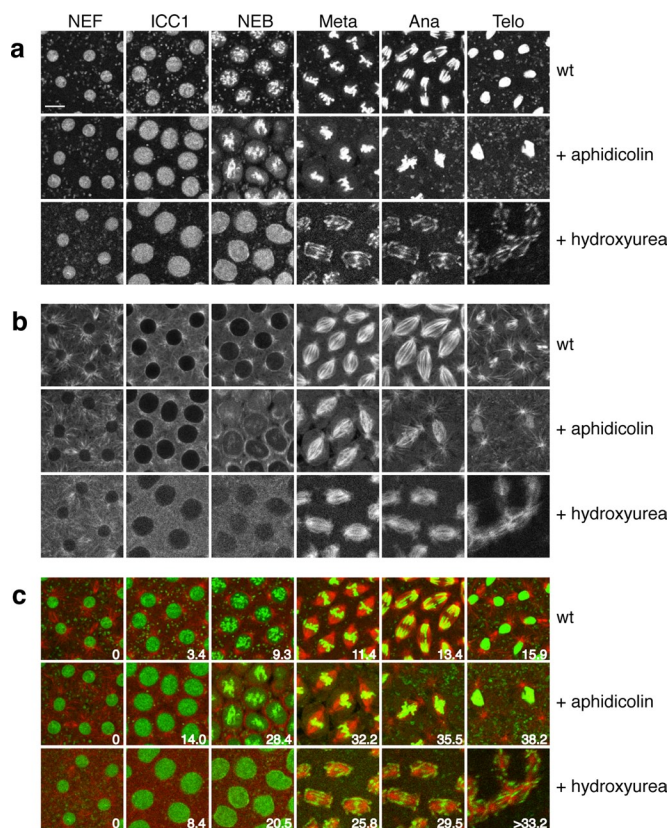


FIGURE 2: Distinct effects of S-phase inhibitors aphidicolin and hydroxyurea on chromosome and microtubule dynamics. Images from embryos injected with these S-phase inhibitors during metaphase of cycle 11 and monitored live through nuclear cycle 12. (A) GFP-histone, (B) rhodamine-tubulin injected, and (C) merge (GFP-histone in green and rhodamine-tubulin in red). Aphidicolin, 0.295 mM; hydroxyurea, 10 mM. Time is shown in minutes. Scale bar, 8 μ m.

14 and to >8.4 min after NEF, respectively (Table 1). These findings suggest a previously unidentified dependence: normal timing of the initiation of chromosome condensation requires a normal S phase (Figure 6).

Although the S-phase inhibitors aphidicolin and hydroxyurea produced similar effects on the timing of chromosome condensation, they exhibited distinct effects on chromosome morphology. In aphidicolin-treated embryos, the chromosomes at NEB were more diffuse and undercondensed relative to the chromosomes observed at the same stage in untreated embryos (Figure 2). It is surprising that in aphidicolin-treated embryos, chromosome condensation and congression on the metaphase plate were relatively normal, with chromosomes appearing slightly hypercondensed. In contrast, hydroxyurea-treated embryos exhibited little evidence of chromosome condensation at NEB. Furthermore, congression and compaction of the chromosomes on the metaphase plate were severely disrupted (Figures 2 and 7).

DNA-damaging agents produced only minor delays in ICC1. The timing of ICC1 was not delayed in x-irradiated embryos and was only slightly delayed in mechlorethamine- and cisplatin-treated embryos (Table 1 and Figure 6).

Each of these three DNA-damaging agents produced distinct effects on chromosome morphology (Figure 3). In x-irradiated embryos at NEB, the chromosomes condensed but were severely disorganized. At metaphase, chromosome congression and alignment on the metaphase plate were relatively normal. In cisplatin-treated embryos at NEB, the chromosomes exhibited a diffuse morphology, indicating a failure in condensation. At metaphase, congression on the metaphase plate occurred, but condensation was severely disrupted. In mechlorethamine-treated embryos at NEB, the condensing chromosomes tended to remain clustered at the nuclear envelope. However, at metaphase, chromosome congression and condensation were only slightly disrupted.

The topoisomerase inhibitors and poisons (aclarubicin, ICRF-193, VM-26, doxorubicin, and camptothecin) also produced only minor delays in ICC1 (1.5- to 2-fold) relative to the S-phase inhibitors (>3-fold; Table 1 and Figure 6).

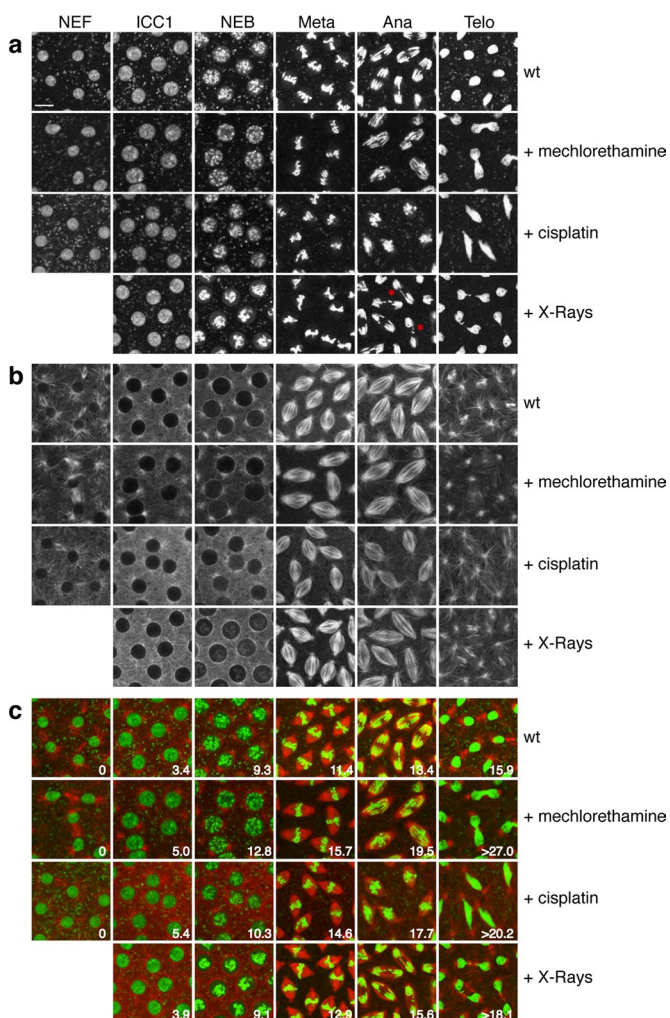
Each topoisomerase drug produced a distinct effect on chromosome condensation. In aclarubicin-treated embryos at NEB, the chromosomes remained inappropriately attached to the nuclear envelope, with a phenotype similar to that found with mechlorethamine (Figure 4). At metaphase, chromosome condensation occurred relatively normally, but congression and alignment on the metaphase plate were severely disrupted. Doxorubicin-treated embryos produced chromosome condensation phenotypes similar to those observed for aclarubicin: chromosomes were inappropriately associated with the nuclear envelope but showed only mild disruptions in organization at metaphase (Figure 5). In ICRF-193-treated embryos at NEB, the chromosomes inappropriately clustered in the center of the nucleus but produced only subtle disruptions in chromosome organization at metaphase (Figure 4). VM26 and camptothecin produced the most severe disruptions in chromosome organization. At NEB, chromosomes did not appear properly condensed, and at metaphase, the organization of the chromosomes on the metaphase plate was severely disrupted (Figure 5).

This analysis indicates that the severity of the chromosome defects at NEB does not correlate with the severity of chromosome defects at metaphase. This is best illustrated by doxorubicin, which severely disrupted chromosome condensation and organization at NEB but resulted in a surprisingly normal chromosome configuration at metaphase (Figure 5).

	Interphase NEF-NEB	Prophase			Metaphase NEB-IA
		NEF-CC2	NEF-ICC1	ICC1-CC2	
Wild type (n = 7)	9.3 ± 0.7	6.4 ± 1.0	3.4 ± 0.5	3.0 ± 1.0	4.1 ± 0.6
+ aphidicolin (n = 5)	28.4 ± 3.7	22.4 ± 4.5	14.0 ± 4.1	8.4 ± 2.3	7.1 ± 1.2
+ ICRF-193 (n = 10)	10.2 ± 2.1	9.1 ± 2.5	5.8 ± 2.4	3.3 ± 0.8	8.0 ± 3.3
+ VM26 (n = 6)	11.4 ± 1.8	>6.7	4.6 ± 0.8	>2.10	>10.5
+ x-rays (n = 10)	10.0 ± 1.4	6.0 ± 0.4	4.5 ± 0.3	1.5 ± 0.2	5.1 ± 0.8
<i>grapes</i> (n = 8)	6.8 ± 1.0	6.2 ± 1.3	3.8 ± 0.5	2.4 ± 1.0	5.7 ± 3.1
+ aphidicolin (n = 6)	6.4 ± 1.3	7.1 ± 1.6	—	—	24 ± 6.9
+ ICRF-193 (n = 7)	6.6 ± 0.8	5.7 ± 0.3	3.8 ± 0.3	1.9 ± 0.2	8.9 ± 3.5
+ VM26 (n = 6)	6.1 ± 1.2	4.5 ± 0.4	2.8 ± 0.4	1.7 ± 0.3	8.3 ± 1.2
+ x-rays (n = 8)	7.4 ± 1.2	6.2 ± 1.0	4.7 ± 0.7	1.6 ± 0.5	6.1 ± 1.2
<i>dwee1</i> (n = 8)	4.0 ± 0.5	3.9 ± 0.3	3.1 ± 0.6	1.0 ± 0.4	4.4 ± 0.4
+ aphidicolin (n = 6)	4.7 ± 0.6	6.1 ± 1.0	—	—	5.0 ± 1.2
+ ICRF-193 (n = 6)	4.7 ± 0.4	4.9 ± 0.6	3.5 ± 0.9	1.7 ± 0.5	6.1 ± 0.9
+ VM26 (n = 6)	3.7 ± 0.6	3.4 ± 0.3	2.3 ± 0.4	1.1 ± 0.2	5.9 ± 1.9
+ x-rays (n = 9)	5.2 ± 0.7	5.3 ± 0.2	4.5 ± 0.3	0.9 ± 0.2	4.3 ± 0.6

Syncytial nuclear cycle 12 was followed in wild-type and *grp-* and *dwee1*-derived embryos bearing the histone-GFP construct. The following intervals were timed (in minutes): NEF to NEB, NEF to ICC, ICC1 to ICC2, and NEB to IA (see the text). x-Rays, 340 rad. n, number of embryo observed. —, not observed. Values are ±SD.

TABLE 2: Nuclear cycle timing in wild-type and *grp-* and *dwee1*-derived drug-treated and untreated embryos.



DNA replication and topoisomerase inhibitors reduce the rate of chromosome condensation in a *Grp/Chk1*- and *dWee1*-dependent manner

To determine whether the delay in the rate of chromosome condensation is checkpoint mediated, we measured this interval in *grp-* and *dwee1*-derived embryos. In aphidicolin-treated, *grp-* and *dwee1*-derived embryos, the interval between NEF and CC2 is 7.1 and 6.1 min, respectively, less than three times that of wild type-treated embryos. These studies demonstrate that *Grp* and *dWee1* mediate the aphidicolin-induced delay in the rate of chromosome condensation (Table 2).

The topoisomerase inhibitor ICRF-193 delays both the initiation and rate of chromosome condensation, although not as dramatically as observed for aphidicolin (Table 2 and Figure 6). In untreated embryos, the interval between NEF and CC2 is ~6.4 min. In ICRF-193-treated embryos, this interval is 9.1 min. Of significance, in ICRF-193-treated, *grp-* and *dwee1*-derived embryos the interval between NEF and CC2 is 5.7 and 4.9 min, respectively. These studies further support our conclusion that *Grp* and *dWee1* mediate the inhibitor-induced delays in chromosome condensation.

The topoisomerase-induced metaphase delays are *dWee1* dependent

Metaphase, defined as the interval between NEB and initiation of anaphase (NEB-IA), lasts 4.1 min in untreated embryos. All of the

FIGURE 3: Distinct effects of DNA-damaging agents cisplatin, mechlorethamine, and x-rays on chromosome and microtubule dynamics. Images from embryos treated with these DNA-damaging agents during metaphase of nuclear cycle 11 and monitored live through nuclear cycle 12. (A) GFP-histone, (B) rhodamine-tubulin injected, and (C) merge (GFP-histone in green and rhodamine-tubulin in red). Mechlorethamine, 10 mM; cisplatin, 1 mM; x-rays, 410 rad. Red asterisks show DNA breaks. Time is shown in minutes. Scale bar, 8 μ m.

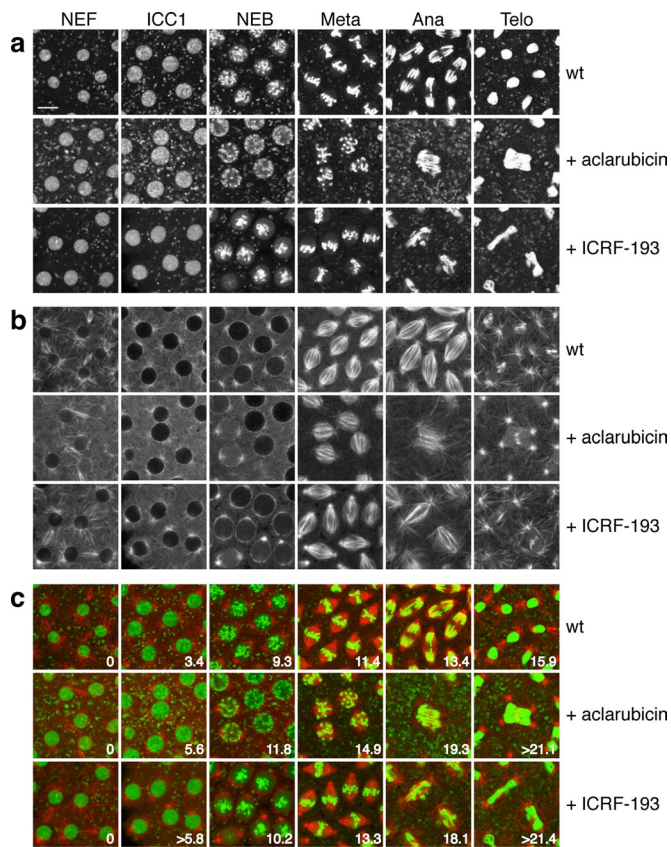


FIGURE 4: Distinct effects of topoisomerase II inhibitors aclarubicin and ICRF-193 on chromosome and microtubule dynamics. Images from embryos treated with these inhibitors during metaphase of nuclear cycle 11 and monitored live through nuclear cycle 12. (A) GFP-histone, (B) rhodamine-tubulin injected, and (C) merge (GFP-histone in green and rhodamine-tubulin in red). Aclarubicin, 10 mM; ICRF-193, 0.5 mM. Time is shown in minutes. Scale bar, 8 μ m.

inhibitors produced substantial delays in metaphase, ranging from 6.5 to >10.5 min. The two inhibitors that produce the most severe defects in chromosome organization on the metaphase plate—the S-phase inhibitor hydroxyurea and the topoisomerase inhibitor VM26—also produce the longest delays in metaphase: >9.0 and 10.5 min, respectively (Table 1 and Figure 6). In addition, these inhibitors induced pronounced disruptions in spindle organization (Figure 7).

A potential explanation for the metaphase delay is the activation of the spindle checkpoint as a result of damaged kinetochores (Mikhailov *et al.*, 2002). Alternatively, the delay might be the result of the activation of DNA damage/structure checkpoints acting at metaphase (Royou *et al.*, 2005). Our analysis of the effects of the *grp* and *dwee1* mutations on this delay, described later, support the latter explanation. To assay whether *dwee1* or *grp* is required for the metaphase delays induced by condensation defects, we injected the topoisomerase II poison VM26 into *grp*- and *dwee1*-deficient embryos. When injected in wild-type embryos, VM26 produces severe disruptions in chromosome condensation and an extremely pronounced metaphase delay (the length of metaphase increases from 4.1 to >10.5 min; Table 2). In four of the six embryos studied, the delay was >15 min.

In contrast, injecting VM26 into *dwee1*-derived embryos did not produce a pronounced increase in metaphase length (uninjected, 4.4 min; injected, 5.9 min). None of the six injected *dwee1* embryos

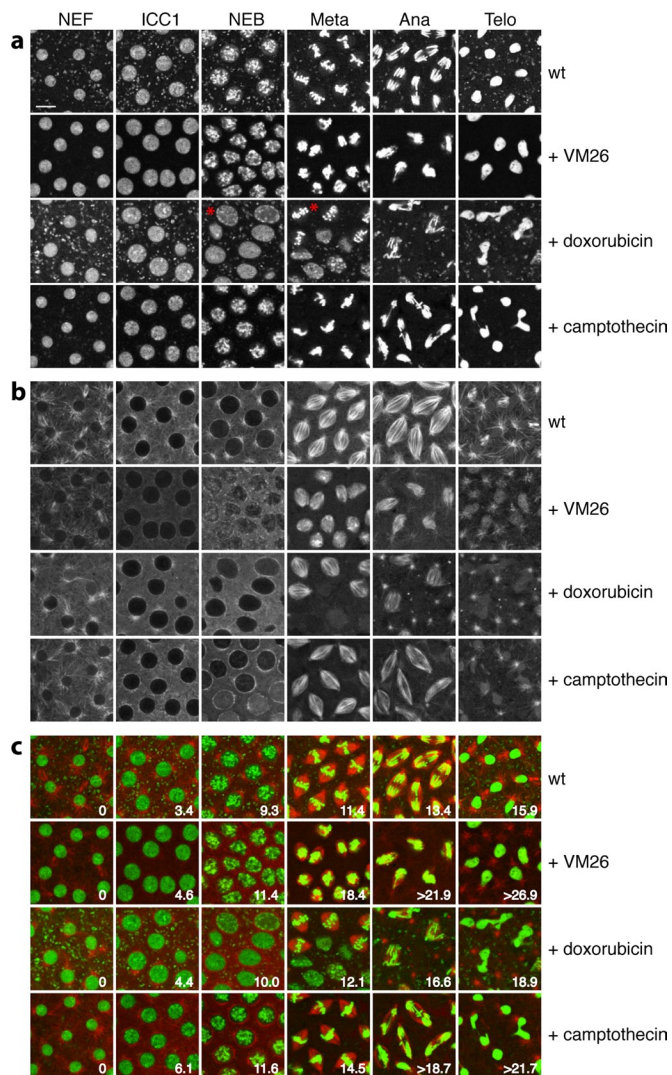


FIGURE 5: Distinct effects of topoisomerase II poisons VM26 and doxorubicin and topoisomerase I poison camptothecin on chromosome and microtubule dynamics. Images from embryos treated with these inhibitors during metaphase of nuclear cycle 11 and monitored live through nuclear cycle 12. (A) GFP-histone, (B) rhodamine-tubulin injected, and (C) merge (GFP-histone in green and rhodamine-tubulin in red). VM26, 0.25 mM; doxorubicin, 0.01 mM; camptothecin, 1.0 mM. Red asterisks indicate the same nucleus from NEB to Meta. Time is shown in minutes. Scale bar, 8 μ m.

produced a delay of >6.2 min. Injecting VM26 into *grp*-derived embryos increased the length of metaphase (from 5.7–8.3 min). Although the elimination of the VM26-induced metaphase delay was not as dramatic as in *dwee1*-derived embryos, it appears that Grp reduces the delay as well.

Loss of dWee1 activity does not disrupt the spindle assembly checkpoint

One possible explanation for the VM26-induced metaphase delay in *dwee1* mutants is that the spindle checkpoint is compromised. In wild-type embryos, injection of colchicine, a microtubule inhibitor, activates the spindle assembly checkpoint, resulting in prolonged metaphase arrest. We observed a similar metaphase arrest when colchicine was injected into *dwee1*-derived embryos, thus demonstrating that the spindle assembly checkpoint is functional

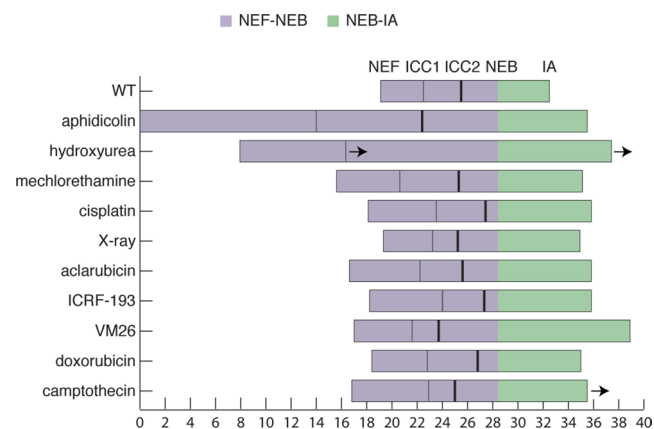


FIGURE 6: Timed intervals for wild-type and drug-treated embryos during syncytial cycle 12. Embryos treated with these inhibitors during metaphase of nuclear cycle 11 and the effect on timing recorded during nuclear cycle 12. The intervals shown are as follows: NEF to ICC1 (gray vertical line), ICC1 to ICC2 (dark vertical line), and ICC2 to NEB and NEB to IA (green interval). The bars of the graph are aligned vertically at NEB. The arrows indicate that the preceding intervals can sometime last for unlimited time. Time is shown in minutes at the bottom of the graph.

in *dwee1*-mutant embryos (Supplemental Figure S2). These results indicate that the absence of the metaphase delay is not due to the loss of the spindle assembly checkpoint.

DISCUSSION

The timing of chromosome condensation is enforced by *dWee1* and *Grp* checkpoint kinases

Previous studies suggest there is a link between DNA replication and chromosome condensation (Pflumm, 2002). Exploring this relationship in precellularized *Drosophila* embryos, we found that injection of the S-phase inhibitors aphidicolin and hydroxyurea produce pronounced delays in both the initiation and rate of chromosome condensation. Initiation of chromosome condensation normally occurs 3.4 min after NEF. In aphidicolin-treated embryos, initiation does not occur until 14 min after NEF. Similar results are obtained with hydroxyurea. Live analysis enabled us to define a second stage of condensation in which the condensing chromosomes pull away from the nuclear envelope. This normally occurs 6.3 min after NEF. In aphidicolin-treated embryos, this second stage is delayed until 22.4 min after NEF, indicating the rate of chromosome condensation is delayed as well.

These data demonstrate that in the early *Drosophila* embryo the timing of initiation and the rate of chromosome condensation depend on S phase. A possible explanation is based on the observation that in addition to inhibiting DNA polymerase, aphidicolin inactivates a subset of replication origins (Marheineke and Hyrien, 2001). Models have been proposed linking the density of replication origins to the degree of lengthwise chromosomal condensation. The DNA protruding from replication complexes generates loops of replicon length, resulting in chromosome condensation. Reducing the number of functional replication origins may result in the observed delays in chromosome condensation. We favor another explanation, however, because although we find a delay in condensation, ultimately the chromosomes condense and congress normally to the metaphase plate. Therefore we pursued the alternative explanation: enforcement of this dependence via cell cycle checkpoints.

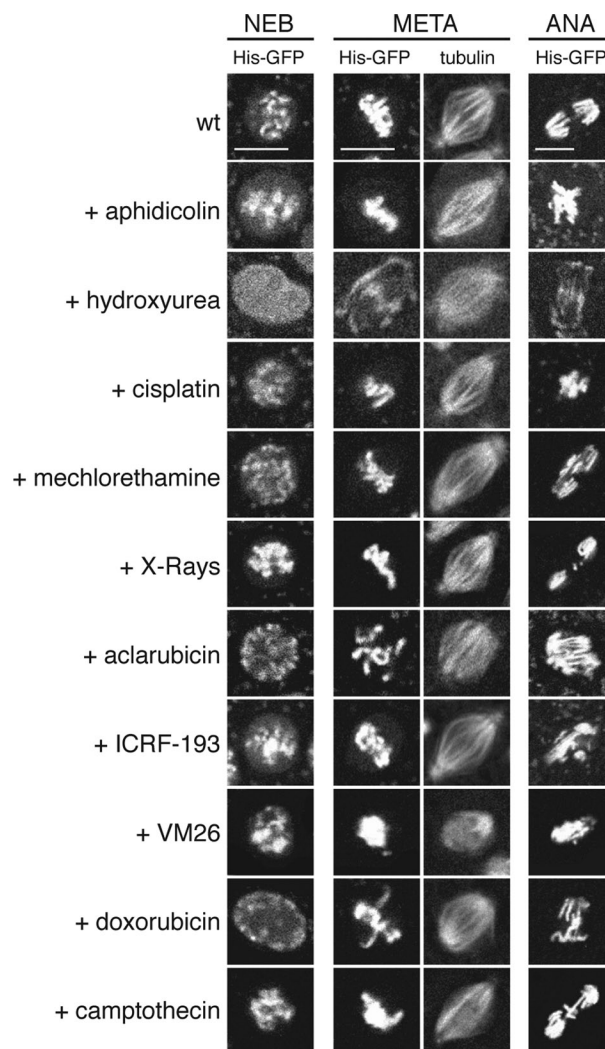


FIGURE 7: Chromatin and microtubule organization in drug-treated and irradiated embryos. Left, the phenotype at NEB of a single nucleus in each drug-treated embryo. Middle two, the spindle and chromosome phenotypes at metaphase. Right, the phenotype at anaphase. Scale bar, 8 μ m.

To test the role played by cell cycle checkpoints in monitoring chromosome condensation, we analyzed the relationship between S phase and chromosome condensation in *grp*- and *dwee1*-mutant embryos. *grp* (*chk1*) and *dwee1* (*wee1*) are essential kinases of the S-phase checkpoint in the syncytial *Drosophila* embryo (Fogarty *et al.*, 1997; Sibon *et al.*, 1997; Price *et al.*, 2000). In wild-type, *grp*, and *dwee1* aphidicolin-treated embryos the second stage of chromosome condensation is 22.4, 7.1, and 6.1 min respectively. These results demonstrate that *Grp* and *dWee1* kinases are required for the aphidicolin-induced delays in condensation. Evidence for this mechanism of enforcement comes from studies demonstrating that in response to unreplicated DNA, *Grp* is required to prevent nuclear import of cyclins (Jin *et al.*, 1996; Royou *et al.*, 2008). Cyclin import is necessary for proper chromosome condensation (Gong and Ferrell, 2010). Therefore, in response to unreplicated chromosomes, *Grp* inhibits cyclin accumulation in the nucleus, preventing chromosome condensation (Royou *et al.*, 2008). According to this model, loss of *Grp* facilitates cyclin import and rapid chromosome condensation. In *Schizosaccharomyces pombe* and *Xenopus*, *Chk1* functions as a positive regulator of *Wee1* kinases (O'Connell *et al.*, 1997;

Lee *et al.*, 2001). Both Chk1 and Wee1 promote inhibition of the Cdk1 mitotic kinase that coordinates early mitotic events, including chromosome condensation (Abe *et al.*, 2011).

We also performed similar experiments using the topoisomerase II (topo II) inhibitor ICRF-193. ICRF-193 specifically inhibits topo II by trapping the enzyme on the DNA in the closed-clamp form (Roca *et al.*, 1994). It is surprising that this only produces a minor increase in S-phase length. However, this treatment does produce significant delays in both stages of chromosome condensation. To our knowledge, this is the first study examining effect of topo II inhibitors on the timing of chromosome condensation. The ICRF-193-induced delay in chromosome condensation is eliminated in *grp* and *dwee1* mutants, indicating that this delay is also enforced by these checkpoints.

Evidence for a dWee1-dependent condensation checkpoint regulating anaphase entry

The spindle assembly checkpoint is viewed as the primary checkpoint controlling the metaphase-to-anaphase transition. Unbound kinetochores or kinetochores with reduced tension result in the activation of the spindle checkpoint, preventing activation of the anaphase-promoting complex (APC) and anaphase entry (Kim and Yu, 2011). It is now clear that DNA damage produces metaphase as well as interphase delays. Both the spindle checkpoint and Grp/Chk1 mediate these delays. Kinetochores damaged by DNA-damaging agents such as x-irradiation activates the spindle checkpoint, but DNA damage to nonkinetochore regions produces metaphase delays that are mediated by Grp/Chk1 (Mikhailov *et al.*, 2002; Royou *et al.*, 2005). Here we provide evidence for a distinct checkpoint at metaphase that monitors the state of DNA condensation. Our analysis reveals a strong correlation between chromosome organization at metaphase and timing of anaphase entry: the more pronounced the condensation defect, the greater is the delay. For example, the inhibitors that produce the most pronounced defects in chromosome condensation—hydroxyurea, VM26, and aclarubicin—also produce extensive metaphase delays. Given that these inhibitors also disrupt S phase and cause DNA damage, this effect could be the result of entering metaphase with damaged or unreplicated DNA rather than specifically due to condensation defects. However, aphidicolin-injected embryos result in pronounced interphase delays, whereas metaphase length is only slightly affected. Furthermore, the chromosomes appear aligned and well condensed on the metaphase plate. Similarly, x-irradiation does not produce chromosome condensation defects and does not exhibit metaphase delays. We therefore believe that much of the metaphase delay observed in embryos treated with topoisomerase inhibitors is the result of chromosome condensation defects. These results are in accord with previous studies showing metaphase delays in *grp/chk1*-mutant embryos. The reduced interphase length in these embryos does not provide sufficient time for proper chromosome condensation, and metaphase is consequently delayed (Yu *et al.*, 2000).

Taken together, these studies show a strong correlation between chromosome condensation defects and the activation of a checkpoint that prevents entry into anaphase. In addition, our studies demonstrate anaphase entry is delayed in *grp/chk1*- but not *dwee1*-mutant embryos upon inhibition of chromosome condensation. Thus dWee1, but not Grp/Chk1, is required for this checkpoint. This result is surprising because dWee1 is an inhibitory kinase that functions during interphase to inhibit Cdk1 activity. Preventing exit from metaphase requires maintaining Cdk1 in an active state. It is possible that dWee1 delays mitotic exit by targeting the APC complex.

Alternatively, there may be a novel mitotic checkpoint that relies on regulation of Cdk1 by inhibitory phosphorylation, as suggested by recent studies in mammalian cells (Jin *et al.*, 1998; Potapova *et al.*, 2009; Chow *et al.*, 2011).

Cytological profiling cell cycle inhibitors in the early *Drosophila* embryo

The inhibitors described here are widely used in basic and clinical research; however, little is known about the cytological consequences and effects of these compounds on cell cycle timing. We exploit our ability to perform live analysis of the rapid divisions of the early *Drosophila* embryo to follow the initial morphological and timing defects induced by the injected compounds (Table 3). In addition, zygotic transcription is greatly reduced in the early embryo, enabling us to directly determine the effects of the drugs on the cell cycle. These studies demonstrate that different drugs that target the same cellular processes or components often produce distinct cytological phenotypes with respect to morphology and cell cycle timing. For example, doxorubicin and VM26 (topoisomerase II poisons) and ICRF-193 (topoisomerase II inhibitor) all target topoisomerase II, but they produce distinct phenotypes of chromosome organization during prophase, metaphase, and anaphase, as well as distinct effects on spindle morphology. At NEB, VM26 results in abnormal chromosome clustering in the center of the nucleus, whereas doxorubicin results in chromosomes gathered along the nuclear envelope.

Similarly, of the two S-phase inhibitors studied, only hydroxyurea produces severe defects in chromosome condensation and congression and spindle organization. In addition, hydroxyurea produces severe defects in the organization of the cortical actin cytoskeleton (Supplemental Figure S3). These results are particularly interesting, given that a side effect of hydroxyurea, often used in treating sickle-cell anemia, is the production of large binucleate vascular endothelial cells (Ballas *et al.*, 1989; Adragna *et al.*, 1994; De Franceschi and Corroche, 2004). Binucleate cells are a classic phenotype of failed cytokinesis that relies on actomyosin-based contraction (Somma *et al.*, 2002). The unique cytological and temporal profiles defined here for commonly used anticancer drugs and cell cycle inhibitors will provide a reference for rapidly classifying the *in vivo* cell cycle effects of new compounds.

MATERIALS AND METHODS

Drosophila stocks

The following stocks were used in this study: w^{1118} ; $P[w^{+mC} = His2Av^{T:Avic[GFP-S65T]}62A$, kindly provided by Robert Saint (Clarkson and Saint, 1999), and *GFP-moe*, kindly provided by Daniel Kiehart (Edwards *et al.*, 1997). *yw; grp¹/CyO; His-GFP/+; w; dwee1^{ES1}/CyO; His-GFP/His-GFP; w; dwee1^{WO5}/CyO; His-GFP/His-GFP. dwee1^{ES1} and dwee1^{WO5} were previously described (Price *et al.*, 2000; Stumpff *et al.*, 2004). *grp¹* was previously described (Sullivan *et al.*, 1993; Fogarty *et al.*, 1994, 1997; Yu *et al.*, 2000). *mei41^{RT1}* (Yamamoto *et al.*, 1990) was kindly provided by R. Scott Hawley, Stowers Institute for Medical Research, Kansas City, MO.*

For analysis of *dwee1* mutants, heterozygous *dwee1^{ES1}* females were crossed with heterozygous *Df(2L)dwee1^{WO5}* males. The hemizygous *dwee1^{ES1}/Df(2L)dwee1^{WO5}* females were then crossed with Oregon-R males. For analysis of *grp¹* mutants, homozygous *grp¹* females were crossed with Oregon-R males.

Materials

To standardize our analysis of the effects of inhibitors on the cell cycle, we injected each inhibitor during metaphase (between NEB and IA) of nuclear cycle 11 and imaged the embryos from telophase of nuclear

Drugs	Interphase	Icc1	Chromosome condensation defects			Sister chromatid bridges	Free chromosome fragments	Spindle defects
			NEB	Metaphase	Metaphase			
Aphidicolin, 0.295 mM	Significantly delayed	Significantly delayed	Severe	Mild	Slightly delayed	Yes	No	None
Hydroxyurea, 10 mM	Significantly delayed	Significantly delayed	Severe	Severe	Significantly delayed	Yes	No	Severe
Cisplatin, 1 mM	Normal	Delayed	Slight	Mild	Delayed	Yes	Yes	Slight
Mechlorethamine, 10 mM	Delayed	Slightly delayed	Slight	Slight	Slightly delayed	Yes	No	Slight
x-Rays, 410 rad	Normal	Normal	None	None	Slightly delayed	Yes	Yes	None
Aclarubicin, 10 mM	Slightly delayed	Delayed	Mild	Mild	Delayed	Yes	No	Slight
ICRF-193, 0.5 mM	Normal	Delayed	Severe	Severe	Delayed	Yes	No	Slight
VM26, 0.25 mM	Slightly delayed	Slightly delayed	Severe	Severe	Significantly delayed	Yes	No	Severe
Doxorubicin, 0.01 mM	Normal	Slightly delayed	Severe	Mild	Slightly delayed	Yes	No	Slight
Camptothecin, 1 mM	Slightly delayed	Delayed	Mild	Mild	Delayed	Yes	Yes	None

TABLE 3: Phenotypes observed in drug-treated and untreated embryos.

cycle 11 through telophase of nuclear cycle 12 (Supplemental Figure S1). The initial concentration used for each inhibitor was obtained from the literature and an ongoing study in our lab aimed at determining the minimal dose that reduces adult survival (Simon *et al.*, 2000; Radcliffe *et al.*, 2002). With this as a starting concentration, we identified an inhibitor concentration that did not result in abnormalities in chromosome segregation or spindle morphology during the anaphase immediately following the injection (anaphase of nuclear cycle 11) but did produce abnormalities during nuclear cycle 12. To further ensure functional equivalence in inhibitor concentration, we choose a concentration at which a 5- to 20-fold-lower concentration produced no obvious abnormalities during nuclear cycles 11 and 12. For example, injecting cisplatin at 0.1 mM produces no abnormalities during nuclear cycle 11 or 12 (Supplemental Figure S1, a). Performing the same injection at 1 mM allowed the nuclei to progress normally through anaphase of nuclear cycle 11, but dramatic segregation defects are observed during anaphase of nuclear cycle 12 (Supplemental Figure S1, b). Finally, performing the same experiments at 10 mM results in immediate abnormalities in chromosome segregation during the anaphase of nuclear cycle 11 (Supplemental Figure S1, c). By obtaining this effective intermediate concentration, we were able to analyze the effects of the drug on morphological as well as timing aspects of the cell cycle. In addition, we were able to analyze the effect of these inhibitors in cell cycle checkpoint-compromised backgrounds.

The following drugs and concentrations were tested: aphidicolin, 0.295 mM; hydroxyurea, 1, 10, and 15 mM; cisplatin, 0.1, 1, and 10 mM; mechlorethamine, 1 and 10 mM; aclarubicin, 4.4 and 10 mM; ICRF-193, 0.03, 0.5, and 1 mM; VM26, 0.0625, 0.25, and 5 mM; doxorubicin, 0.001, 0.01, and 0.1 mM; and camptothecin, 0.1 and 1 mM. The concentration chosen for each drug and the solvent used are as follows: aphidicolin, 0.295 mM, 2% dimethyl sulfoxide (DMSO) in H₂O; hydroxyurea, 10 mM, 10% DMSO in H₂O; mechlorethamine, 10 mM, 10% DMSO in H₂O; cisplatin, 1 mM in H₂O; aclarubicin, 10 mM in H₂O; doxorubicin, 0.01 mM, 0.1% DMSO in H₂O;

ICRF-193, 0.5 mM, 5% DMSO in H₂O; VM26, 0.25 mM, 5% DMSO in H₂O; camptothecin, 1 mM, 4% DMSO in H₂O; x-rays, 340 and 410 rad. The x-ray treatment was performed with a Torrex 120D machine (Astrophysics Research, City of Industry, CA). The dechorionated embryos were first irradiated and immediately after were placed on the stage of the confocal microscope for observation. The concentration of colchicine injected in *dwee1* embryos was 0.5 mM, 19.2% DMSO in H₂O. The drugs were obtained from the following sources: mechlorethamine, Developmental Therapeutics Program at the National Cancer Institute (Rockville, MD); ICRF-193, Biomol (Enzo Life Sciences, Plymouth, PA); and aphidicolin, hydroxyurea, cisplatin, aclarubicin, VM26, camptothecin, doxorubicin, and colchicine, Sigma-Aldrich (St. Louis, MO).

Live-embryo analysis

Embryos were prepared for microinjection and time-lapse scanning confocal microscopy as previously described (Tram *et al.*, 2001). Rhodamine-labeled tubulin was purchased from Molecular Probes (Invitrogen, Carlsbad, CA) and Cytoskeleton (Denver, CO).

Microscopy

Microscopy was performed using an inverted photoscope (DMIRB; Leitz, Leica, Wetzlar, Germany) equipped with a laser confocal imaging system (TCS SP2; Leica) with an HCX PL APO CS 63.0x, 1.32, oil objective (Leica). Leica confocal software, version 2.6.1, and Photoshop CS5 (Adobe, San Jose, CA) were used for the image processing. Movies were assembled using QuickTime Pro 7 (Apple, Cupertino, CA). For furrow expansion analysis, time-lapse confocal images were taken of GFP-moesin-expressing embryos from NEF to NEB of cycle 12. A Z series was taken every 2.5 μm.

Adult survival assays

Inhibitor-spiked medium is created by heating a standard cornmeal and molasses medium until boiling. The medium is stirred until the

temperature drops to <55°C, at which time the drug is stirred in. The medium is then poured into vials and seeded with wild-type embryos and mutant larva. The adult flies are collected and counted.

ACKNOWLEDGMENTS

We thank Chris Field, Ulrike Eggert, Giorgia Siriaco, and members of the Sullivan and Kellogg laboratories for helpful discussions and critical reading of the manuscript. This work was supported by a grant to W.S. from the National Institutes of Health (GM44757) and a grant to B. F. from the University of California Institute for Quantitative Biomedical Research, as well as a grant from the Canadian Institutes of Health Sciences to S.D.C.

REFERENCES

- Abe S, Nagasaka K, Hirayama Y, Kozuka-Hata H, Oyama M, Aoyagi Y, Obuse C, Hirota T (2011). The initial phase of chromosome condensation requires Cdk1-mediated phosphorylation of the CAP-D3 subunit of condensin II. *Genes Dev* 25, 863–874.
- Adragna NC, Fonseca P, Lauf PK (1994). Hydroxyurea affects cell morphology, cation transport, and red blood cell adhesion in cultured vascular endothelial cells. *Blood* 83, 553–560.
- Baker JM, Parish JH, Curtis JP (1984). DNA-DNA and DNA-protein cross-linking and repair in *Neurospora crassa* following exposure to nitrogen mustard. *Mutat Res* 132, 171–179.
- Ballas SK, Dover GJ, Charache S (1989). Effect of hydroxyurea on the rheological properties of sickle erythrocytes in vivo. *Am J Hematol* 32, 104–111.
- Breger KS, Smith L, Thayer MJ (2005). Engineering translocations with delayed replication: evidence for cis control of chromosome replication timing. *Hum Mol Genet* 14, 2813–2827.
- Chow JP, Poon RY, Ma HT (2011). Inhibitory phosphorylation of cyclin-dependent kinase 1 as a compensatory mechanism for mitosis exit. *Mol Cell Biol* 31, 1478–1491.
- Clarkson M, Saint R (1999). A His2AvDGFP fusion gene complements a lethal His2AvD mutant allele and provides an in vivo marker for *Drosophila* chromosome behavior. *DNA Cell Biol* 18, 457–462.
- Coelho PA, Queiroz-Machado J, Sunkel CE (2003). Condensin-dependent localisation of topoisomerase II to an axial chromosomal structure is required for sister chromatid resolution during mitosis. *J Cell Sci* 116, 4763–4776.
- Cuvier O, Hirano T (2003). A role of topoisomerase II in linking DNA replication to chromosome condensation. *J Cell Biol* 160, 645–655.
- De Franceschi L, Corroche R (2004). Established and experimental treatments for sickle cell disease. *Haematologica* 89, 348–356.
- Edwards KA, Demsky M, Montague RA, Weymouth N, Kiehart DP (1997). GFP-moesin illuminates actin cytoskeleton dynamics in living tissue and demonstrates cell shape changes during morphogenesis in *Drosophila*. *Dev Biol* 191, 103–117.
- Foe VE, Alberts BM (1983). Studies of nuclear and cytoplasmic behaviour during the five mitotic cycles that precede gastrulation in *Drosophila* embryogenesis. *J Cell Sci* 61, 31–70.
- Fogarty P, Campbell SD, Abu-Shumays R, Phalle BS, Yu KR, Uy GL, Goldberg ML, Sullivan W (1997). The *Drosophila* grapes gene is related to checkpoint gene *chk1/rad27* and is required for late syncytial division fidelity. *Curr Biol* 7, 418–426.
- Fogarty P, Kalpin RF, Sullivan W (1994). The *Drosophila* maternal-effect mutation grapes causes a metaphase arrest at nuclear cycle 13. *Development* 120, 2131–2142.
- Gong D, Ferrell JE Jr (2010). The roles of cyclin A2, B1, and B2 in early and late mitotic events. *Mol Biol Cell* 21, 3149–3161.
- Gotoh E (2007). Visualizing the dynamics of chromosome structure formation coupled with DNA replication. *Chromosoma* 116, 453–462.
- Hatzl VI, Terzoudi GI, Paraskevopoulou C, Makropoulos V, Matthopoulos DP, Pantelias GE (2006). The use of premature chromosome condensation to study in interphase cells the influence of environmental factors on human genetic material. *ScientificWorldJournal* 6, 1174–1190.
- Jin P, Gu Y, Morgan DO (1996). Role of inhibitory CDC2 phosphorylation in radiation-induced G2 arrest in human cells. *J Cell Biol* 134, 963–970.
- Jin P, Hardy S, Morgan DO (1998). Nuclear localization of cyclin B1 controls mitotic entry after DNA damage. *J Cell Biol* 141, 875–885.
- Johnson RT, Rao PN (1970). Mammalian cell fusion: induction of premature chromosome condensation in interphase nuclei. *Nature* 226, 717–722.
- Kim S, Yu H (2011). Mutual regulation between the spindle checkpoint and APC/C. *Semin Cell Dev Biol* 22, 551–558.
- Kotadia S, Crest J, Tram U, Riggs B, Sullivan W (2010). Blastoderm formation and cellularization in *Drosophila melanogaster*. *Encyclopedia of Life Sciences*, Chichester, United Kingdom: John Wiley & Sons, http://bio.research.ucsc.edu/people/sullivan/pdf/Kotadia_2010.pdf.
- Laurencon A, Purdy A, Sekelsky J, Hawley RS, Su TT (2003). Phenotypic analysis of separation-of-function alleles of MEI-41, *Drosophila* ATM/ATR. *Genetics* 164, 589–601.
- Lee J, Kumagai A, Dunphy WG (2001). Positive regulation of Wee1 by Chk1 and 14-3-3 proteins. *Mol Biol Cell* 12, 551–563.
- Lundgren K, Walworth N, Booher R, Dembski M, Kirschner M, Beach D (1991). mik1 and wee1 cooperate in the inhibitory tyrosine phosphorylation of cdc2. *Cell* 64, 1111–1122.
- Marheineke K, Hyrien O (2001). Aphidicolin triggers a block to replication origin firing in *Xenopus* egg extracts. *J Biol Chem* 276, 17092–17100.
- McKnight SL, Miller OL Jr (1976). Ultrastructural patterns of RNA synthesis during early embryogenesis of *Drosophila melanogaster*. *Cell* 8, 305–319.
- Mikhailov A, Cole RW, Rieder CL (2002). DNA damage during mitosis in human cells delays the metaphase/anaphase transition via the spindle-assembly checkpoint. *Curr Biol* 12, 1797–1806.
- Nghiem P, Park PK, Kim Y, Vaziri C, Schreiber SL (2001). ATR inhibition selectively sensitizes G1 checkpoint-deficient cells to lethal premature chromatin condensation. *Proc Natl Acad Sci USA* 98, 9092–9097.
- Niida H, Tsuge S, Katsuno Y, Konishi A, Takeda N, Nakanishi M (2005). Depletion of Chk1 leads to premature activation of Cdc2-cyclin B and mitotic catastrophe. *J Biol Chem* 280, 39246–39252.
- O’Connell MJ, Raleigh JM, Verkade HM, Nurse P (1997). Chk1 is a wee1 kinase in the G2 DNA damage checkpoint inhibiting cdc2 by Y15 phosphorylation. *EMBO J* 16, 545–554.
- Pflumm MF (2002). The role of DNA replication in chromosome condensation. *Bioessays* 24, 411–418.
- Pflumm MF, Botchan MR (2001). Orc mutants arrest in metaphase with abnormally condensed chromosomes. *Development* 128, 1697–1707.
- Potapova TA, Daum JR, Byrd KS, Gorbosky GJ (2009). Fine tuning the cell cycle: activation of the Cdk1 inhibitory phosphorylation pathway during mitotic exit. *Mol Biol Cell* 20, 1737–1748.
- Price D, Rabinovitch S, O Farrell PH, Campbell SD (2000). *Drosophila* wee1 has an essential role in the nuclear divisions of early embryogenesis. *Genetics* 155, 159–166.
- Radcliffe CM, Silva EA, Campbell SD (2002). A method for assaying the sensitivity of *Drosophila* replication checkpoint mutants to anti-cancer and DNA-damaging drugs. *Genome* 45, 881–889.
- Roca J, Ishida R, Berger JM, Andoh T, Wang JC (1994). Antitumor bis-dioxopiperazines inhibit yeast DNA topoisomerase II by trapping the enzyme in the form of a closed protein clamp. *Proc Natl Acad Sci USA* 91, 1781–1785.
- Royou A, Gagou ME, Karess R, Sullivan W (2010). BubR1- and Polo-coated DNA tethers facilitate poleward segregation of acentric chromatids. *Cell* 140, 235–245.
- Royou A, Macias H, Sullivan W (2005). The *Drosophila* grp/chk1 DNA damage checkpoint controls entry into anaphase. *Curr Biol* 15, 334–339.
- Royou A, McCusker D, Kellogg DR, Sullivan W (2008). Grapes(Chk1) prevents nuclear CDK1 activation by delaying cyclin B nuclear accumulation. *J Cell Biol* 183, 63–75.
- Samoshkin A, Arnautov A, Jansen LE, Ouspenski I, Dye L, Karpova T, McNally J, Dasso M, Cleveland DW, Strunnikov A (2009). Human condensin function is essential for centromeric chromatin assembly and proper sister kinetochore orientation. *PLoS One* 4, e6831.
- Shermoen AW, McClelland ML, O Farrell PH (2010). Developmental control of late replication and S phase length. *Curr Biol* 20, 2067–2077.
- Sibon OC, Stevenson VA, Theurkauf WE (1997). DNA-replication checkpoint control at the *Drosophila* midblastula transition. *Nature* 388, 93–97.
- Simon JA, Szankasi P, Nguyen DK, Ludlow C, Dunstan HM, Roberts CJ, Jensen EL, Hartwell LH, Friend SH (2000). Differential toxicities of anti-cancer agents among DNA repair and checkpoint mutants of *Saccharomyces cerevisiae*. *Cancer Res* 60, 328–333.
- Smits VA, Klompmaaker R, Arnaud L, Rijkse G, Nigg EA, Medema RH (2000). Polo-like kinase-1 is a target of the DNA damage checkpoint. *Nat Cell Biol* 2, 672–676.

- Somma MP, Fasulo B, Cenci G, Cundari E, Gatti M (2002). Molecular dissection of cytokinesis by RNA interference in *Drosophila* cultured cells. *Mol Biol Cell* 13, 2448–2460.
- Song YH (2005). *Drosophila melanogaster*: a model for the study of DNA damage checkpoint response. *Mol Cells* 19, 167–179.
- Stumpff J, Duncan T, Homola E, Campbell SD, Su TT (2004). *Drosophila* Wee1 kinase regulates Cdk1 and mitotic entry during embryogenesis. *Curr Biol* 14, 2143–2148.
- Sullivan W, Fogarty P, Theurkauf W (1993). Mutations affecting the cytoskeletal organization of syncytial *Drosophila* embryos. *Development* 118, 1245–1254.
- Tram U, Riggs B, Koyama C, Debec A, Sullivan W (2001). Methods for the study of centrosomes in *Drosophila* during embryogenesis. *Methods Cell Biol* 67, 113–123.
- van Vugt MA, Smits VA, Klompmaker R, Medema RH (2001). Inhibition of Polo-like kinase-1 by DNA damage occurs in an ATM- or ATR-dependent fashion. *J Biol Chem* 276, 41656–41660.
- Woodcock CL, Ghosh RP (2010). Chromatin higher-order structure and dynamics. *Cold Spring Harb Perspect Biol* 2, a000596.
- Yamamoto AH, Brodberg RK, Banga SS, Boyd JB, Mason JM (1990). Recovery and characterization of hybrid dysgenesis-induced mei-9 and mei-41 alleles of *Drosophila melanogaster*. *Mutat Res* 229, 17–28.
- Yu KR, Saint RB, Sullivan W (2000). The Grapes checkpoint coordinates nuclear envelope breakdown and chromosome condensation. *Nat Cell Biol* 2, 609–615.
- Zhai L, Wang H, Tang W, Liu W, Hao S, Zeng X (2011). Disturbance in function and expression of condensin affects chromosome compaction in HeLa cells. *Cell Biol Int* 35, 735–740.